AFRL-AFOSR-VA-TR-2022-0155

Towards Inserting Magnetic Ejecta into a Space Weather Model

De Koning, Curt
REGENTS OF THE UNIVERSITY OF COLORADO
3100 MARINE ST 572 UCB
BOULDER, CO,
US

05/19/2022
Final Technical Report

Air Force Research Laboratory
Air Force Office of Scientific Research
Arlington, Virginia 22203
Air Force Materiel Command

REPORT DOCUMENTATION PAGE

PLEASE DO NOT RETURN YOUR FORM TO THE ABOVE ORGANIZATION.

1. REPORT DATE	2. REPORT TYPE	3. DATES COVERED	
20220519	Final	START DATE 20140930	END DATE 20210929

4. TITLE AND SUBTITLE
Towards Inserting Magnetic Ejecta into a Space Weather Model

5a. CONTRACT NUMBER	5b. GRANT NUMBER	5c. PROGRAM ELEMENT NUMBER
	FA9550-14-1-0401	61102F
5d. PROJECT NUMBER	**5e. TASK NUMBER**	**5f. WORK UNIT NUMBER**

6. AUTHOR(S)
Curt De Koning

7. PERFORMING ORGANIZATION NAME(S) AND ADDRESS(ES)
REGENTS OF THE UNIVERSITY OF COLORADO
3100 MARINE ST 572 UCB
BOULDER, CO
US

8. PERFORMING ORGANIZATION REPORT NUMBER

9. SPONSORING/MONITORING AGENCY NAME(S) AND ADDRESS(ES)	10. SPONSOR/MONITOR'S ACRONYM(S)	11. SPONSOR/MONITOR'S REPORT NUMBER(S)
Air Force Office of Scientific Research 875 N. Randolph St. Room 3112 Arlington, VA 22203	AFRL/AFOSR RTB1	AFRL-AFOSR-VA-TR-2022-0155

12. DISTRIBUTION/AVAILABILITY STATEMENT
A Distribution Unlimited: PB Public Release

13. SUPPLEMENTARY NOTES

14. ABSTRACT
Our objective is to investigate and characterize magnetic structures within CMEs, from eruption to impact with Earth, using a combination of data-supported models and enhanced remote sensing data that connect solar and in-situ measurements. Although the magnetic field entrained in a CME is critical to its geoeffectiveness, predicting that field has been difficult because of incomplete understanding and modeling limitations; hence, current forecasting tools do not account for CME magnetic field. Satisfying our objective will improve space weather prediction through new physical understanding and through the tools we develop. Our project meets key scientific and operational goals of AFOSR by advancing basic research and the goal of a geoeffectiveness forecast capability. Our work is organized to address specific questions: 1. How are CME magnetic structures observed near the Sun connected to in-situstructures? By measuring the structural and kinematic evolution of CME cavities (flux ropes) in enhanced white-light images from STEREO, which enable continuous tracking and association of solar and in-situ structures, we will gain understanding of how CME magnetic structures evolve from Sun to Earth, and enable better prediction of CME geoeffectiveness. 2. What are the dynamics of CMEs in interplanetary space? With a few innovative changes to WSA-Enlil, we will produce simulations of hypothetical magnetic ejecta, leading to understanding of solar wind interactions, and directly enabling a better CME geoeffectiveness forecast capability. 3. How does CME behavior in the solar wind change with differing physical circumstances surrounding its launch? Using a novel hybrid simulation designed to preserve magnetic structure, we will investigate CME launch scenarios and their affect on CME evolution, and compare them with enhanced imaging data from STEREO. This will lead to understanding of the origins of CME structure observed at Earth, and enable better prediction of CME geoeffectiveness based on near-surface solar observations.

15. SUBJECT TERMS

16. SECURITY CLASSIFICATION OF:			17. LIMITATION OF ABSTRACT	18. NUMBER OF PAGES
a. REPORT U	b. ABSTRACT U	c. THIS PAGE U	UU	18

19a. NAME OF RESPONSIBLE PERSON	19b. PHONE NUMBER *(Include area code)*
JULIE MOSES	426-9586

Towards Inserting Magnetic Ejecta Into a Space Weather Model

PI: Curt A. de Koning *University of Colorado at Boulder/CIRES*

Final performance report

(2014/09/30–2021/09/29)

Award number *FA9550-14-1-0401*

1 Introduction

In the AFOSR-funded project, "Towards Inserting Magnetic Ejecta Into a Space Weather Model," the objective was to investigate and characterize CMEs, including the magnetic field entrained within the CME, from eruption to impact with Earth, using a combination of data-supported models and enhanced remote sensing data that connect solar and in-situ measurements. Satisfying this objective meets key scientific and operational goals of AFOSR by improving space weather prediction through new physical understanding. The project was organized to address several specific questions:

1. How are CME magnetic structures observed near the Sun connected to in-situ structures?
2. What are the dynamics of CMEs in interplanetary space?
3. How does CME behavior in the solar wind change with differing physical circumstances surrounding its launch?

This was a collaborative project completed by the University of Colorado (CU) and the Southwest Research Institute (SWRI). The third question listed above was addressed by researchers at SWRI only; the first two questions were addressed by team members at either institution.

In this report, we highlight the research accomplishments involving de Koning that were funded by AFOSR during the entirety of this project. For completeness, the final report from SWRI is attached to this report.

2 Analysis of CME Magnetic Structure

One of the fundamental results stemming from this project, if not the fundamental result, was the analysis of the magnetic structure entrained within the CME of 2010-04-03. The results of this work were published in the paper "3D Polarized Imaging of Coronal Mass Ejections: Chirality of a CME" by DeForest, de Koning, and Elliott and appeared in the 2017 *Astrophysical Journal*. In addition to this publication in a refereed journal, the result was also presented by de Koning at eight meetings in 2017–2019, including two invited talks.

This work was accomplished using polarized white light images that had been specially processed by SWRI team member DeForest. The ratio of polarized brightness, pB, to total brightness, B, at each pixel measures the out-of-sky-plane scattering location of that pixel. In particular, we estimate the out-of-sky-plane scattering location for each pixel in the inverse-C feature shown in Figure 1. Next, we choose an axis that passes through the geometric center of the reconstructed point cloud; we call this the x-axis. We also choose a plane, the yz-plane, such that the x-axis is normal to this plane. Within this coordinate system, we calculate the x coordinate of each scattering location, and the position angle, θ, of each scattering location projected onto the yz plane. In effect, we are calculating the cylindrical coordinates, x and θ, of each point in the inverse-C feature. Careful examination of the data suggests that a 'nice' linear relationship between x and θ occurs when the x- axis is oriented such that the axis lon = $+40^\circ$ and the axis lat = $+15^\circ$, as shown in Figure 2. Figure 2 indicates that as we move along the inverse-C feature in a counter-clockwise direction – the standard direction of increasing angle in cylindrical coordinates – the scattering

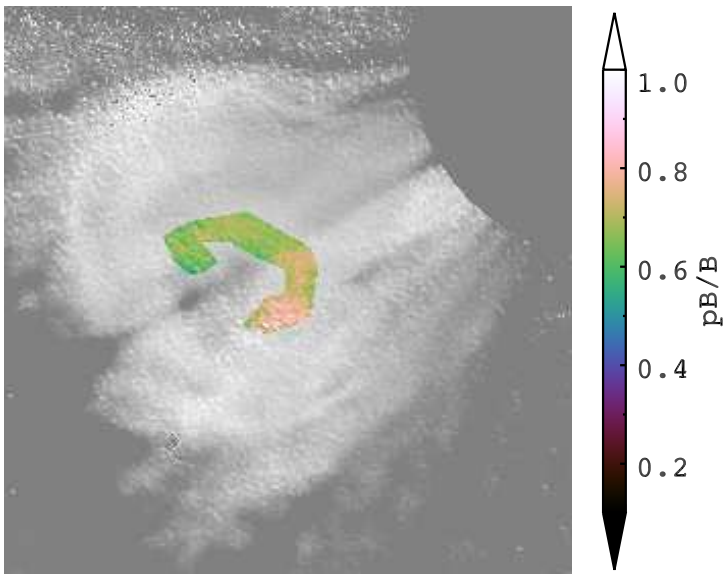

Figure 1: A degree of polarization image calculated from STEREO-A/COR2 data for a CME observed on 2010-04-03 at 11:08:15 UT. Values of pB/B within the inverse-C feature, which is the internal CME region that we are interested in, are quantified according to the color bar on the right. Measurements of pB/B are used to find the three-dimensional spatial locations of each pixel within the inverse-C.

locations move further away from the yz plane; this is indicative of a feature with right-handed morphological chirality.

In addition, we can use the pB/B ratio to estimate the out-of-sky-plane scattering location for each pixel in the CME. We also color-code each reconstructed pixel location by its mass, which is related to the pixel brightness. Next we consider only the least massive portion of the CME, the white-light cavity, and suggest that this (relatively) evacuated portion corresponds to the most magnetically strong portion of the CME, that is, the CME magnetic flux rope. Figure 3 shows the location of the CME flux rope.

Remote measurement of the CME's entrained magnetic structure is an important step toward both understanding CME physics and predicting geoeffectiveness of individual CMEs.

Publications

C. E. DeForest, C. A. de Koning, and H. A. Elliott. 3D Polarized Imaging of Coronal Mass Ejections: Chirality of a CME. *Astrophysical Journal*, 850:130 (8pp), 2017. doi: 10.3847/1538-4357/aa94ca.

Oral Presentations

1. C. A. de Koning& C. E. DeForest. Using Polarized White Light to Unlock the Interior of a CME. At *L5 Consortium Meeting*, Göttingen, Germany, Oct 2017.

2. C. A. de Koning& C. E. DeForest. Using Multi-View Polarimetry to Investigate a CME White-Light Cavity. Invited talk at *Into the Red Dragon's Lair*, Cardiff, Wales, Dec 2017.

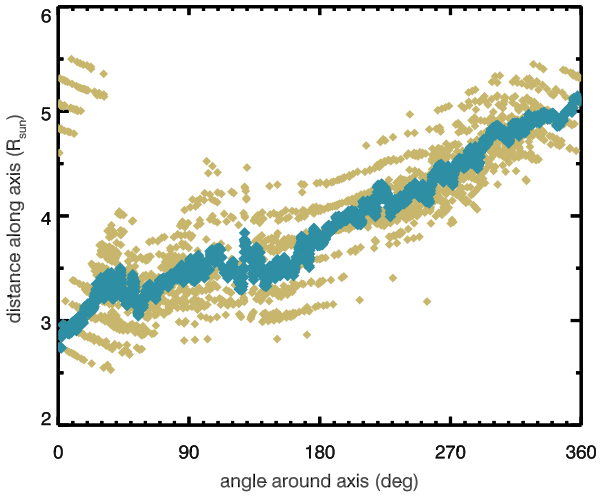

Figure 2: Distance along a spiral axis oriented such that the axis lon = $+40^\circ$ and the axis lat = $+15^\circ$ versus the angular position around the axis for all points within the inverse-C. A counter-clockwise rotation through the inverse-C feature shows that the scattering location increases along the axis; this is indicative of a feature with right-handed morphological chirality.

3. C. A. de Koning& C. E. DeForest. Using STEREO Polarized White-Light Triplets to Reconstruct Features in a CME. At *Fall AGU Meeting*, New Orleans, LA, Dec 2017.

4. C. A. de Koning& C. E. DeForest. Polarimetric Imaging Can Trace Internal CME Features. Invited talk at *NSO Solar Focus Meeting*, Boulder, CO, Jan 2018.

5. C. A. de Koning, D. Odstrcil, & C. E. DeForest. Using Polarized White-Light Triplets Measured by STEREO to Constrain CME Propagation in the Solar Wind. At *Solar Wind 15*, Brussels, Belgium, Jun 2018.

6. C. A. de Koning. Towards Inserting Magnetic Ejecta into a Space Weather Model: The Power of Polarized White Light. At *AFOSR Bz Review*, Albuquerque, NM, Jan 2019.

Poster Presentations

1. C. A. de Koning, D. Odstrcil, & C. E. DeForest. Using Polarized White-Light Triplets Measured by STEREO to Isolate Internal Structure. At *SHINE*, Cocoa Beach, Fl, Jul 2018.

2. C. A. de Koning, C. E. DeForest & D. Odstrcil. In-Depth Analysis of the 2010-04-03 CME. At *Space Weather Workshop*, Boulder, CO, Apr 2019.

3 Challenging Some Contemporary Views of CMEs

As mentioned in the attached SWRI Final Report, Howard and Pizzo [2016] published a paper titled "Challenging Some Contemporary Views of Coronal Mass Ejections. I. The Case for Blast

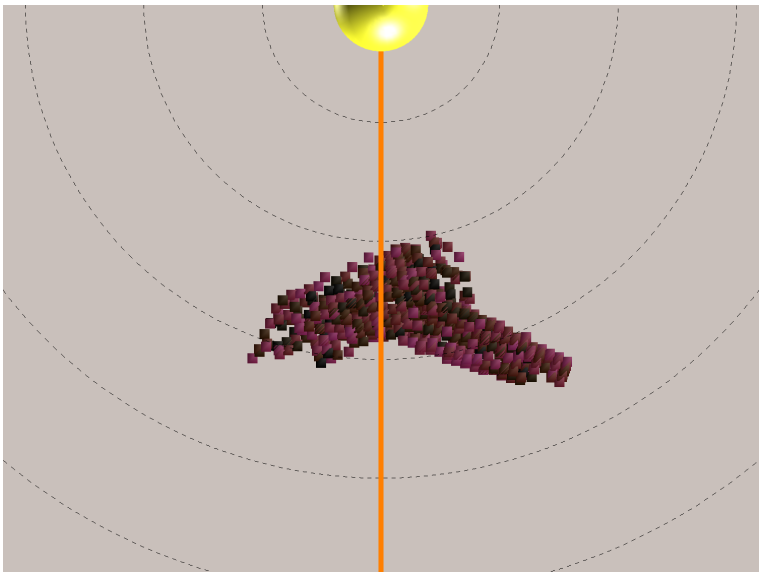

Figure 3: A reconstruction of the white-light cavity of the CME on 2010-04-03. This reconstruction uses data from both STEREO-A and STEREO-B. It shows a view of the white-light cavity looking from solar north down onto the solar equatorial plane.

Waves." In our opinion, this challenge has become necessary since, with the publication of Jack Gossling's seminal paper "The Solar Flare Myth," a certain degree of tunnel vision has affected the space physics community when thinking about CME-related phenomena and their impacts. Howard and Pizzo [2016] presented evidence that some large-scale coronal eruptions, particularly those associated with coronal waves – also known as EIT waves – exhibit characteristics that are more consistent with a blast wave originating from a localized region, such as a flare site, rather than a large-scale structure driven by a CME flux rope.

The challenge is continued by de Koning, Pizzo, and Seaton in a paper titled "The Solar Eruption of 2017 September 10: Wavy with a Chance of Protons" that is nearing publication with the Astrophysical Journal. (Note, the proof of the article has been corrected.) This paper describes a large-scale coronal wave, or blast wave, shown in Figure 4, that originated near NOAA Active Region 12673 during a solar eruption on 2017-09-10. This solar eruption spawned an X8.2 flare, a CME, the just-mentioned blast wave, and strong solar particle emissions, including solar energetic particles (SEPs) and a ground level event (GLE). The wave shown in Figure 4 is part of a larger, dome-shaped wave that eventually encompasses the entire Sun.

Diffusive shock acceleration, which is considered to be the most likely, even dominant, contributor to the production of intense particle events, can take place anywhere along the dome-shaped wave observed during the solar eruption of 2017 September 10; a schematic picture illustrating the dome-shaped wave is shown in Figure 5. The dome-shaped wave is depicted by the multicolored, solid line that surrounds the balloon, labeled 'CME.' The Sun is the gray, marbled region at the bottom of the picture. The various dashed lines represent magnetic field lines, and the two arrows are two shock normals. Particle acceleration along the top of the dome, in the red zone that extends out from the nose of the dome, is usually identified as acceleration by the CME-driven shock. Since the publication of "The Solar Flare Myth," the acceleration of solar protons to relativistic energies, or GLE particles, has been attributed to either direct acceleration during the flare energy release or

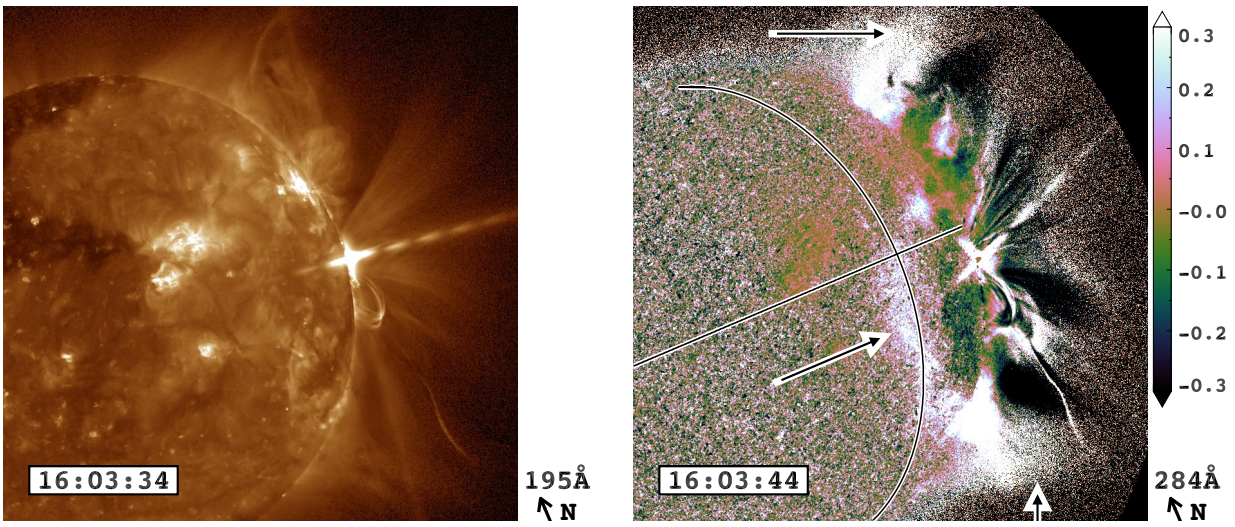

(a) (b)

Figure 4: (a) The large-scale coronal wave detected in the GOES-16 195Å passband at 16:03:34 UT. In this specially-processed intrinsic brightness image, which retains its natural appearance, dynamic features, such as the coronal wave, are visible over the solar limb. (b) The large-scale coronal wave detected in the GOES-16 284Å passband at 16:03:44 UT. Whereas panel (a) showed an intrinsic brightness image, this running relative-difference image has enhanced the leading edge of the wave, especially on the solar disk; the leading-edge of the wave shows up as the broad, curved, white feature indicated by the on-disk arrow. Arrows also indicate the northern and southern extent of the wave in the plane of the sky. According to the color scale to the right of the relative-difference image, the white regions have undergone a $\geq 30\%$ increase in intensity compared to the previous time step. The white/black lines show a circle of latitude – the solar equator – and a circle of longitude – 40° west of the Earth-Sun line. The intersection of these two great circles indicates the nominal footpoint of the Parker spiral magnetic field. The orientation of solar north, in these and all subsequent SUVI images, is shown in the legend at the bottom righthand of the images.

to acceleration by a CME-driven shock wave in the high corona.

In our paper paper we challenge this view and show that a two-step particle acceleration process that starts at the base of the blast wave and continues at the dome of the wave, in the green zone of Figure 5, could also accelerate solar protons to GeV energies. We focused particularly on the first-to-arrive GLE particles that were observed by the Fort Smith neutron monitor. To analyze the intensity-time profile of a neutron monitor, it is important to consider its asymptotic directions of approach, which indicates the location in the outer magnetosphere where particles of a particular energy must have originated to be observed at the neutron monitor in question after gyrating through the magnetosphere. It has been shown that the asymptotic directions of approach for the Fort Smith neutron monitor were well-aligned with the Sun-Earth magnetic field line. Although there were other neutron monitors with relatively nearby asymptotic directions of approach – Inuvik, Nain, Peawanuck – these stations did not see the onset of the GLE until many minutes after it was observed by Fort Smith. This indicates that the initial relativistic particles observed by Fort Smith were confined to a narrow, field-aligned beam. Such a beam suggests a short-lived acceleration mechanism that injects particles directly at the base of the Sun-Earth field line. As described in our paper, one way to achieve such a beam is through a blast wave that accelerates particles in two steps as it sweeps over the Sun-Earth footpoint.

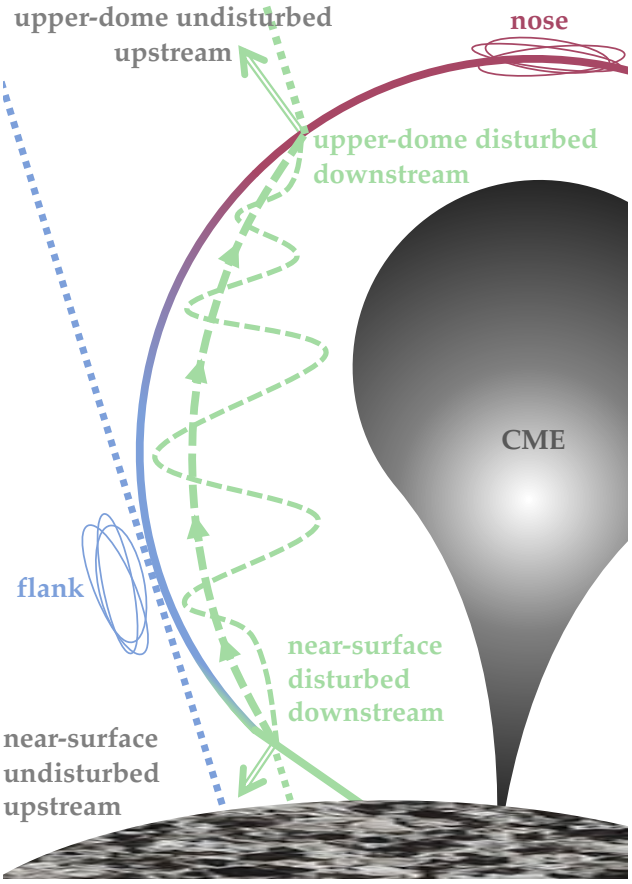

Figure 5: A schematic picture of the large-scale coronal wave or blast wave, which propagates laterally across the solar surface. The gray, marbled region is the Sun; the bubble-like structure extending above the solar surface of the Sun, outlined by the colored, solid line, is the blast wave; the balloon in the right half of the picture is the CME; the various dashed lines represent magnetic field lines; and the two arrows are two shock normals. Note that this schematic is not drawn to scale.

We conclude the paper by acknowledging that there are multiple combinations of transport and acceleration processes that can be postulated to qualitatively match the totality of neutron monitor observations. However, because the relevant indirect evidence is far from being conclusive, it is not straightforward to determine which of these scenarios most closely matches the reality on the Sun. Therefore, as researchers continue to analyze and model past and future GLEs and large SEPs, we urge them to consider all possible acceleration mechanisms that may be operative at the Sun, including the potential role of blast waves – not forgetting the near-surface, refracted portion of the blast wave – as well as those of flares and CME-driven shockwaves.

Publications

C. A. de Koning, V. J. Pizzo, and D. B. Seaton. The Solar Eruption of 2017 September 10: Wavy with a Chance of Protons. *Astrophysical Journal*, 2021. In publication.

Oral Presentations

1. C. A. de Koning, V. Pizzo & D. Seaton. 2017 September 10: Wavy With A Chance of Particles. At *SWPC Seminar*, Boulder, CO, Aug 2019.

2. C. A. de Koning, V. Pizzo & D. Seaton. 2017 September 10: Wavy With A Chance of Particles. **Invited talk** at *SHINE*, Boulder, CO, Aug 2019.

4 Investigating CME Mass

The paper, "Lessons Learned from the Three View Determination of CME Mass" by de Koning appeared in the 2017 *Astrophysical Journal*. In this paper, we discuss the estimation of large-scale CME characteristics, particularly CME mass, as determined from coronagraph observations. Although CMEs are intrinsically three-dimensional structures, they appear as two-dimensional projections when viewed in white-light. With only single-viewpoint total brightness images, such as those from SOHO/LASCO, it is not possible to calculate a true CME mass because total-brightness images do not contain any depth or directional information. Adding a second viewpoint enables calculation of a de-projected CME mass that better approximates the true mass, yet should not be confused with a CME's true mass – because we still assume that the CME is confined to a plane, albeit not the sky plane. Adding a third viewpoint, by exploiting all available perspectives provided by SOHO and STEREO, provides a fresh perspective in calculating CME mass. All together, we use triple-viewpoint analysis to estimate the mass of eight CMEs. In this paper, we highlight two important conclusions learned from this research: First, by requiring that the three independent viewpoints agree, the calculated CME mass will be more accurate than any estimation that relies on two views only. Second, the difficulty in achieving agreement across three independent viewpoints quantifies the uncertainties in the de-projected CME mass.

A thorough uncertainty analysis is a step that is often overlooked in the estimation of CME mass or any large-scale CME characteristic. In fact, in many situations, such as space weather forecasting, the need to quantify uncertainty is more important than the need for increased accuracy.

Publications

C. A. de Koning. Lessons Learned from the Three-view Determination of CME Mass. *Astrophysical Journal*, 844:61 (13pp), 2017. doi: 10.3847/1538-4357/aa7a09.

Poster Presentations

C. A. de Koning. Various Ways to Calculate CME Mass. At *Space Weather Workshop*, Boulder, CO, May 2017.

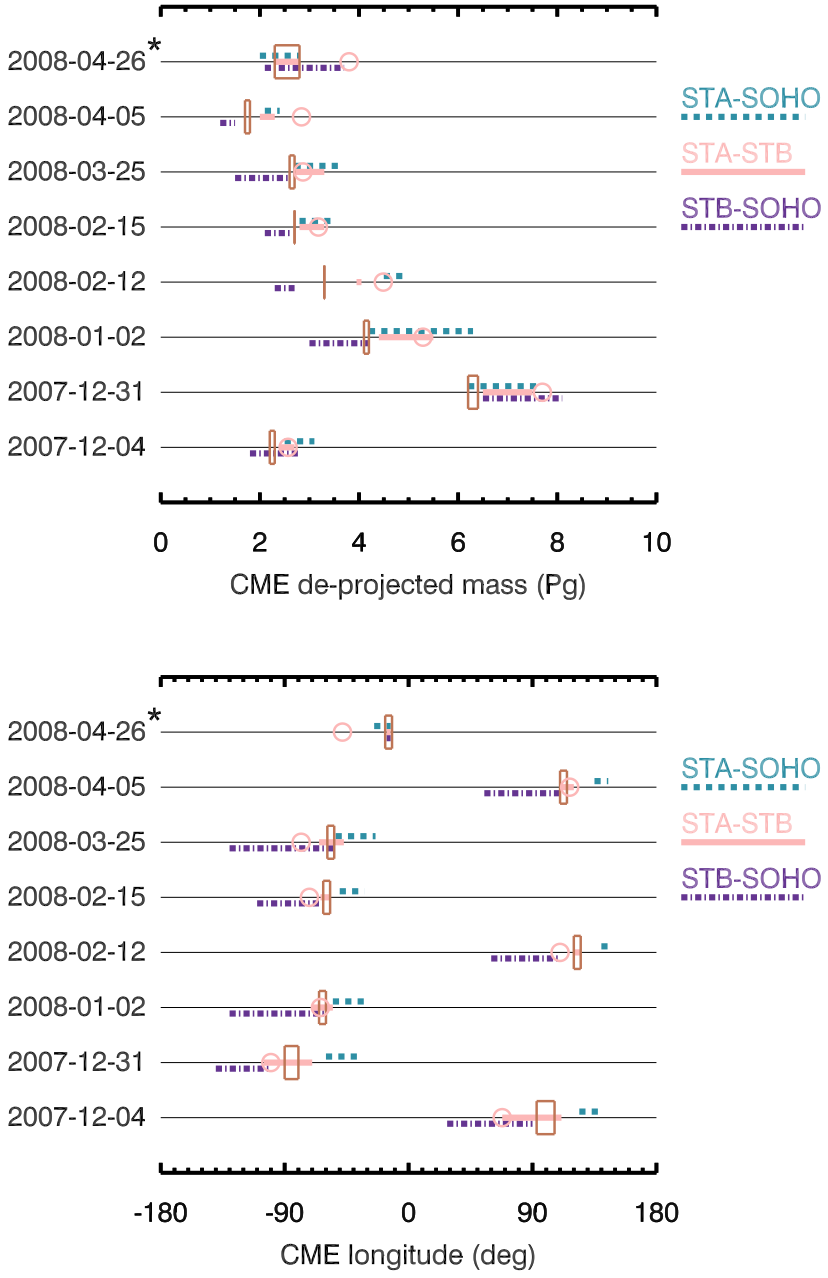

Figure 6: Multi-viewpoint determination of CME de-projected mass (top panel) and longitude of propagation (bottom panel). The blue-green, dashed line shows the region of intersection when comparing observations from STEREO-A (STA) and SOHO. The pink, solid line shows the region of intersection when comparing observations from STEREO-A (STA) and STEREO-B (STB). These values can be directly compared to the results of Colaninno and Vourlidas [2009], shown as pink, open circles. The purple, dashed-dotted line shows the region of intersection when comparing observations from STEREO-B (STB) and SOHO. The brown boxes indicate are the triple viewpoint regions of overlap when both aleatory variation and epistemic uncertainty are considered.

5 CME Dynamics in Interplanetary Space

The research on CME evolution in and transport thru interplanetary space has been done in conjunction with colleagues from the University of Reading in the UK. It has resulted in three papers on which de Koning is a co-author. All the papers deal with using the STEREO Heliospheric Imagers (HIs), especially their potential to improve space weather forecasting.

Usually, STEREO HI data is modeled using simple geometric models, such as Fixed Phi, Harmonic Mean, Self-Similar Expansion, or Elliptic Conversion. Barnard et al. [2017] report that a comparison of CME kinematics estimated independently from the STEREO-A and STEREO-B HI data for four events – 2012-08-31, 2012-09-28, 2012-10-05, and 2012-11-20 – reveals inconsistencies that cannot be explained within the observational errors and model assumptions. Barnard et al. [2017] conclude that these observations imply that the use of the simple, rigid geometric models to represent CME transport through interplanetary space are routinely invalidated and that their utility in a space weather forecasting context is open to question. Using the same four events mentioned above as case studies, Barnard et al. [2020] report that HI observations can be used to improve the skill and reduce the uncertainty of ensemble hindcasts of these events. For these four events, weighted ensembles show a mean reduction in arrival time error of $20 \pm 4\%$ and a mean reduction in arrival time uncertainty of $15 \pm 7\%$ relative to an unweighted ensembles. A key feature of the simple geometric models that are used to model the transport of CMEs in interplanetary space is that a structured solar wind will not affect CME evolution. Barnard et al. [2021] use a large number of CME simulations with a simple solar wind model to quantify the scale of uncertainty introduced into geometric modelling of CME arrival times by solar wind structure. Simulations are produced for an average, fast, and extreme CME propagating through 100 different ambient solar wind backgrounds. Synthetic heliospheric imager observations of these simulations are then used with the standard geometric models mentioned above to estimate the CME kinematics. For these CME scenarios, geometric modelling errors are minimised for an observer in the L5 region. Not surprisingly, geometric modelling errors increase with the level of solar wind structure in the path of the CME.

Publications

1. L. A. Barnard, C. A. de Koning, C. J. Scott, M. J. Owens, J. Wilkinson, and J. A. Davies. Testing the Current Paradigm for Space Weather Prediction with Heliospheric Imagers. *Space Weather*, 15:782–803, 2017. doi: 10.1002/2017SW001609.

2. L. A. Barnard, M. J. Owens, C. J. Scott, and C. A. de Koning. Ensemble CME Modeling Constrained by Heliospheric Imager Observations. *AGU Advances*, 1:e2020AV000214, 2020. doi: 10.1029/2020AV000214.

3. L. A. Barnard, M. J. Owens, C. J. Scott, M. Lockwood, C. A. de Koning, T. Amerstrofer, J. Hinterreiter, C. Möstl, J. A. Davies, and P. Riley. Quantifying the Uncertainty in CME Kinematics Derived from Geometric Modelling of Heliospheric Imager Data. *Space Weather*, 2021. doi: 10.1029/2021SW002841. In Publication.

6 Personnel Supported

- Curt A de Koning – PI
- Dusan Odstrcil – Co-I

7 Program Managers

Original program managers:

- Dr. Kent Miller, AFOSR/RTB;
- Dr. John Luginsland, AFOSR/RTB.

Current program managers:

- Dr. Julie Moses, AFOSR/RTB.

Toward Inserting Magnetic Ejecta Into a Space Weather Model
AFOSR Grant FA9550-14-1-0296
PI: Curt de Koning, CIRES/SWPC
Contract PI: Craig DeForest, SwRI

Final Report, 30 April 2021

Introduction

This research project was part of a larger team effort toward measuring and predicting the intrinsic magnetic field within coronal mass ejections from the Sun. Our team's contribution included observation and analysis of CME substructures, including the flux rope cavity, and the application and improvement of models of CMEs at large distances from the Sun, along with the testing of various physical scenarios involving CME evolution through the solar wind. The work was motivated by the major objective of investigating and characterizing magnetic structures within CMEs from eruption at the Sun to impact with Earth's magnetosphere, using a combination of novel data-supported models and remote sensing data to connect solar and in-situ measurements.

The following report describes the contributions to this project by the contracting team at the Southwest Research Institute. The report describing the contributions by the entire team, including those in *this* report, will be submitted by the PI, Curt de Koning. The contribution by the team at SwRI has involved the analysis and reduction of particular CME datasets and the measurement of their substructure, and development of the fluxon code to be used in Y4 joint simulations.

In 2014, the Air Force Office of Scientific Research (AFOSR) awarded funding to the collaborative grant, ``*Towards Inserting Magnetic Ejecta Into A Space Weather Model*.'' Funding was awarded to research teams at two institutions: (i) University of Colorado at Boulder/Cooperative Institute for Research in Environmental Sciences (CIRES), consisting of Curt A de Koning (Grant PI), Dusan Odstrcil, and George Millward; and (ii) Southwest Research Institute (SWRI) – Boulder, consisting of Timothy Howard (Institutional PI) and Craig DeForest. AFOSR awarded five years of funding to both teams; however, the starting dates for the teams did not coincide — the University of Colorado start date was 9/30/2014, whereas the SWRI start date was 9/1/2014.

In November 2016, SwRI PI Timothy Howard left the field of solar/space physics and returned home to Australia. Howard's departure led to difficulty with the SwRI element of the grant, until the hire and training of Chris Lowder to operate and extend the fluxon code. Nevertheless, we produced several important science results and significantly advanced the technology of fluxon modeling – achieving a major milestone of carrying out meaningful global, data-driven 3D MHD modeling of the corona in the low-beta regime with several orders of magnitude less computer time than would be required for a comparable conventional code.

Accomplishments

In Y1 and Y2 we focused primarily on the analysis goals of the project, culminating in two important papers challenging current understanding of CME onset. In Y1, Howard & Pizzo (2016) made a strong case that blast waves driven by magnetic explosions play an important role in the most energetic CME onset events (Figure 1).

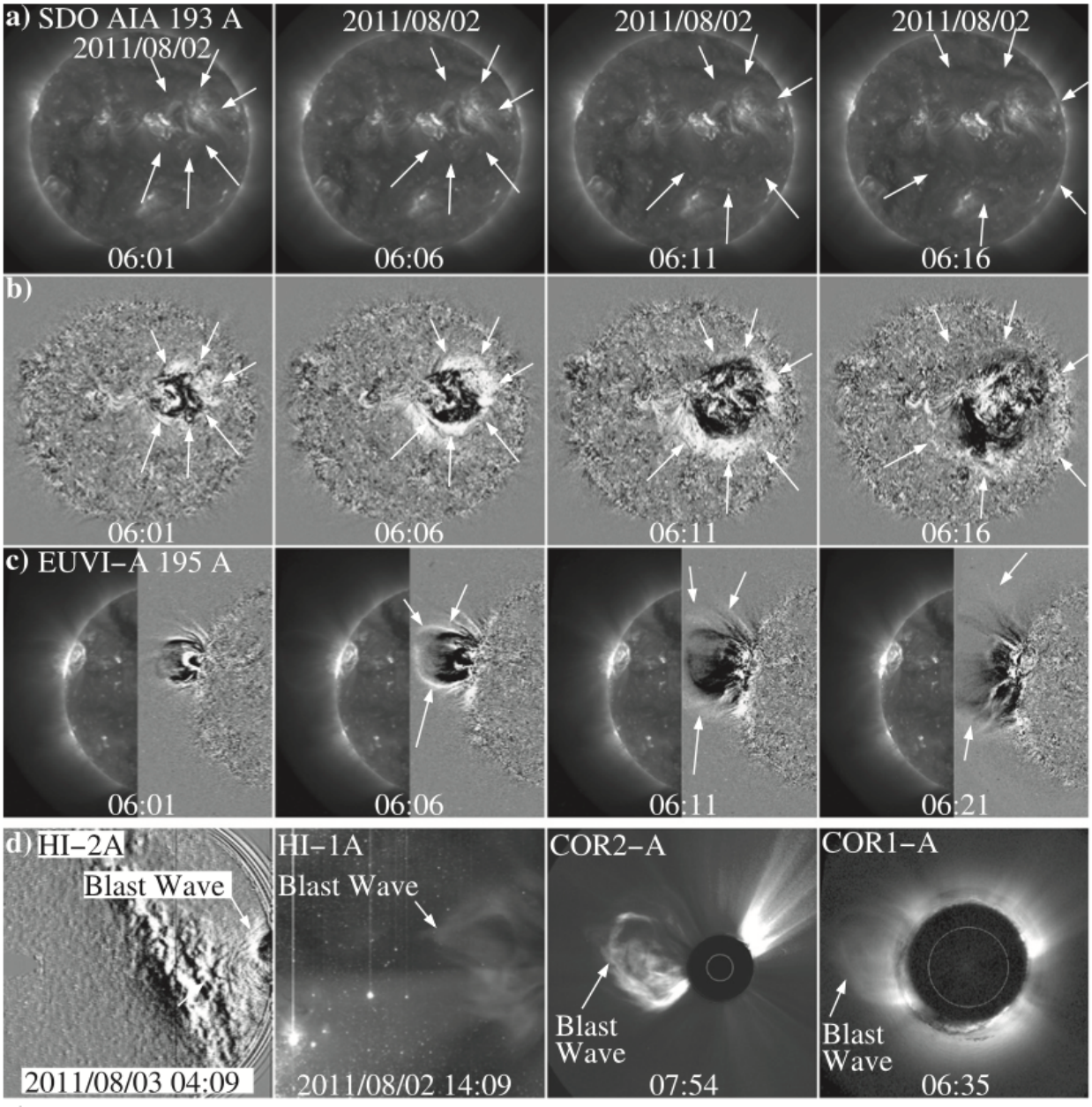

Figure 1 (Fig. 3 of Howard & Pizzo 2016): blast waves from magnetic explosions, despite being downplayed through the field, are important to the physics of the fastest, most energetic CME events.

In Y2, Howard, DeForest, Schneck & Alden (2017) demonstrated that many "filaments" observed in coronagraph movies of CME onset are consistent with optical illusions caused by perspective effects acting on writhed CME flux ropes in the corona (Figure 2). This insight may solve the "case of the missing filaments": cool filamentary material is occasionally observed *in situ* but at much lower rates than the typical three-part CME paradigm would imply. The result shows that filamentary material, whether it erupts in the low corona or not, need not survive to high altitudes to reproduce the appearance of most three-part CMEs in wide-field coronagraphs. The result indicates that filament "evaporation" through conductive heating may influence onset and early propagation more than previously thought, perturbing CME acceleration and affecting model extrapolations of halo CME arrival time.

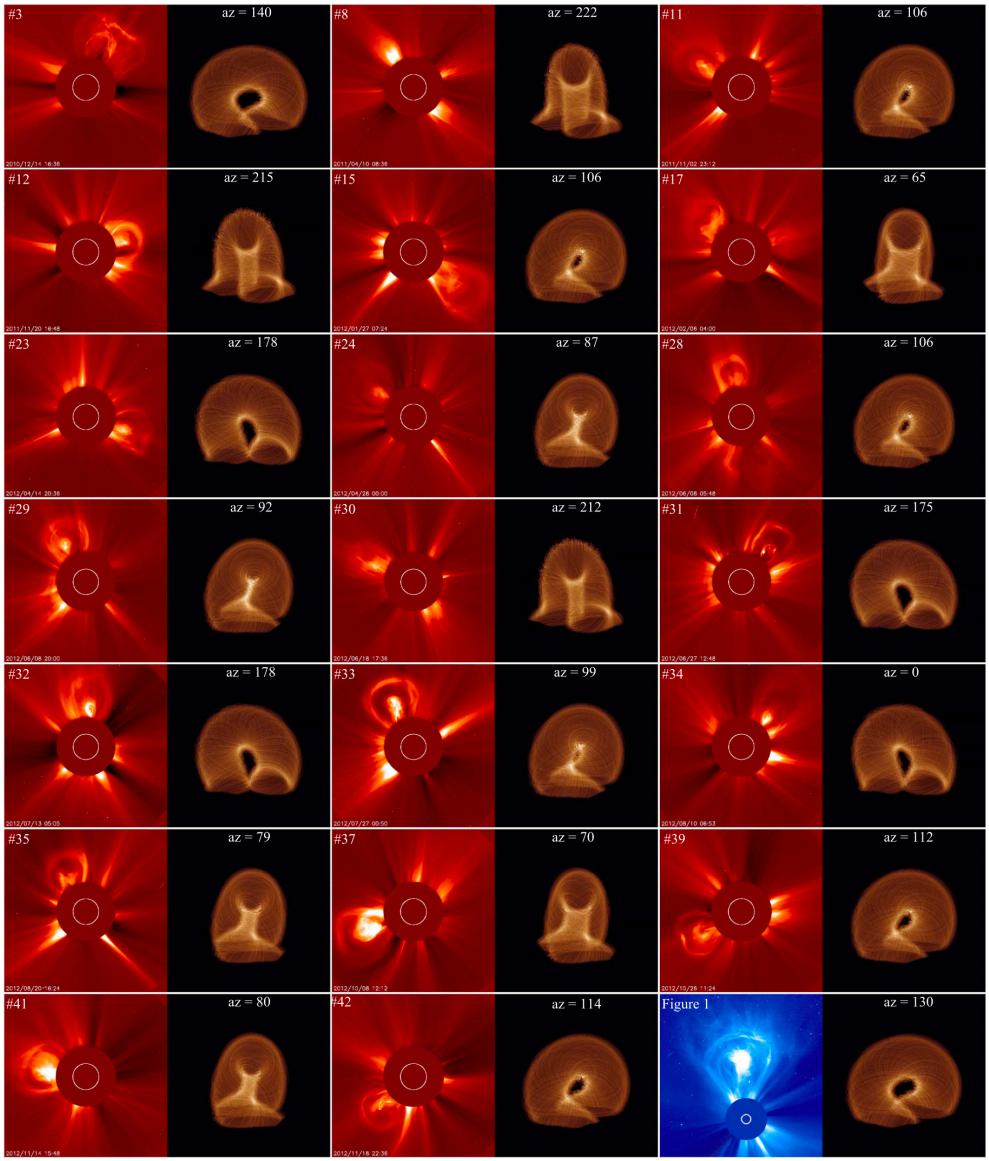

Figure 2 (Fig. 11 of Howard et al. 2017): a simple writhed-flux-rope model, viewed from different angles, substantially reproduces the appearance of many "three-part" CMEs. This implies that some or all "three-part" CMEs may be missing the central "part" (the filament core) in the LASCO C2 or C3 fields of view, potentially explaining the "missing filament" problem of in-situ CME observations.

In Y3 and Y4 we worked with PI De Koning to apply novel noise-reduction techniques to STEREO data and demonstrate the 3D chiral sense of a CME that later impacted SOHO (DeForest, DeKoning & Elliott 2017). This important result demonstrated, for the first time, that visible-light remote sensing of CMEs *as they propagate through interplanetary space*, can determine the chirality (rotational sense) of the flux rope in transit (Figure 3). This, in turn, provides a means to connect now-commonly-available magnetograph measurements of east/west field direction in the CME source region, with extremely important and currently-impossible-to-measure sign of Bz (the north/south component of the CME's entrained magnetic field), through direct measurement rather than modeling. Bz is a critical measurement because it is the single largest determinant of a CME's geoeffectiveness, but it is not currently measurable until the CME sweeps over an *in situ* probe such as ACE or SOHO.

Follow-up work (de Koning & DeForest 2018) revealed that STEREO-B, viewing the CME from the opposite side, placed the structures consistently with the STEREO-A and SOHO results.

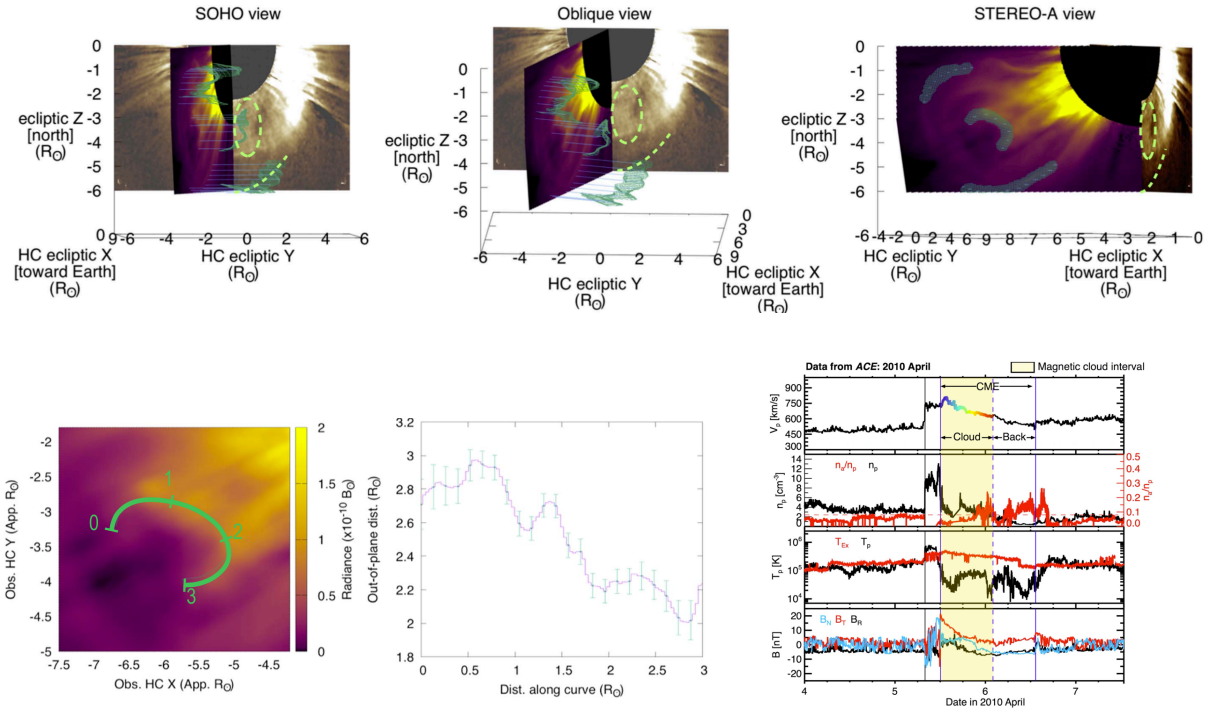

Figure 3: (Figures from DeForest, DeKoning, & Elliott 2017): polarization analysis of a CME demonstrates location of the CME and also determines its chirality. Counterclockwise from top right: (i) CME appears as a clean eastern-limb event from STEREO-A; (ii) oblique view shows green regions-of-interest outside the original image plane based on polarization; (iii) reprojecting to the SOHO point of view aligns the ROI features with SOHO-observed features; (iv) close-up of the core shows a path around the flux rope; (v) path is right-handed helical; (vi) ACE in-situ data confirm right-handed chirality.

In Y4 through Y6, we focused on improving the fluxon simulation code FLUX. FLUX is a quasi-Lagrangian 3D MHD model that is optimized for low-beta-parameter systems such as the lower corona. The model is constructed to use the magnetic field itself as a grid: the magnetic domains of the corona are modeled directly, with curvilinear fluxons (field lines that carry finite, rather than infinitesimal, magnetic flux) that interact via the familiar magnetohydrodynamic (MHD) magnetic pressure and curvature forces. Because magnetic domains are quantized, numerical reconnection is completely eliminated and it is not necessary

to oversample the domain. This reduces the computational requirements for a full-corona model by a factor between 10^3 and 10^4 compared to an Eulerian MHD code of comparable resolution that is capable of capturing the pre-CME flux system.

Because FLUX is the first fluxon model intended to simulate the Sun, the simulation problem has proved more complex than anticipated and major development was needed. In Y4 we carried out programmer-interface improvements, allowing improved interaction with the model and 3D rendering and visualization of the entire corona via Python plot libraries (Figure 4). We also validated the simulation against WSA models of the coronal morphology during particular Carrington rotations.

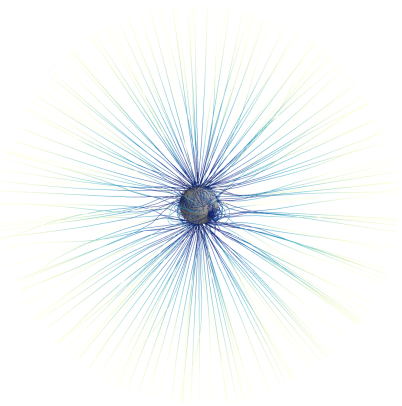

Figure 4: Improved rendering of a global fluxon model shows uniform outer field as expected; reveals connectivity of streamer boundaries and coronal holes to the heliosphere.

In Y5 we added mass flows to the model, in particular enabling simulation of the solar wind environment (Figure 5). We validated stationary flows against WSA and against analytic treatment of several typical open magnetic structures. By the end of Y5 we began to insert closed but unstable flux systems into the model to allow them to erupt – either from toroidal force or from explicit reconnection. We requested a one year No-Cost Extension to enable applying the FLUX code to the team-selected CME events.

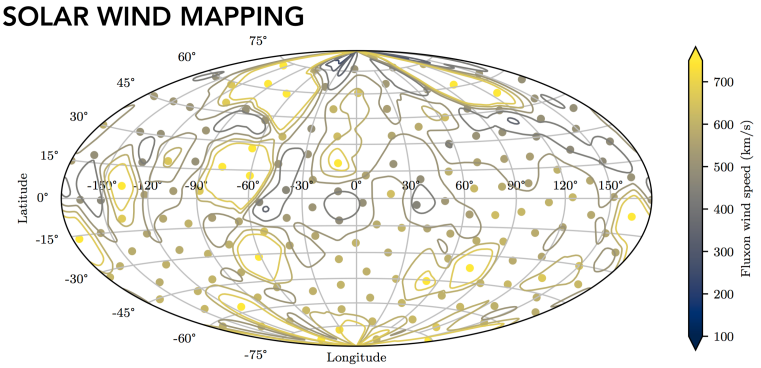

Figure 5: Addition of flow to individual fluxon domains allows prediction of solar wind speed over the entire outer stretch of the corona. This wind model uses a polytropic index and uniform basal temperature; cross sectional morphology of open field lines differentiates fast from slow flows.

In Y6, we encountered several novel numerical difficulties as we scaled up to full-resolution simulation codes. We found that certain models which converged well with 1,000 fluxons did not converge well (or at all) with 3x improved resolution (10,000 fluxons) – let alone with our target density of 100,000 fluxons. After several months of effort we tracked down two separate errors that prevented applying the model to the targeted CMEs at the required resolution. First, models and boundary conditions were being transferred between parallel processes with insufficient numerical precision, leading to occasional "sticky" infinities in the force calculation. This, in turn, froze portions of the model and prevented convergence with high fluxon counts but had no effect at low fluxon counts and therefore was difficult to reproduce under controlled circumstances. To identify and resolve this particular issue we had to develop an entirely new 3D visualization back-end for the code to allow us to trace and browse individual fluxons and their neighborhoods through the simulation. Second, certain aspects of the mass calculation led to new unanticipated numerical instabilities that involved interactions between the cross sectional area around each fluxon and the modeled flow characteristics. We refined the flow code by using a higher order interpolation of the flux tube cross section and also by imposing damping terms to the analytic 1-D treatment of the flow, to prevent the instability. These quasi-viscous terms smooth flow along each field line and help to find the correct solution -- but do not damp shear flows across field lines. The result of these efforts is that we can now automatically produce data-driven wind models at the anticipated resolution (Figure 6).

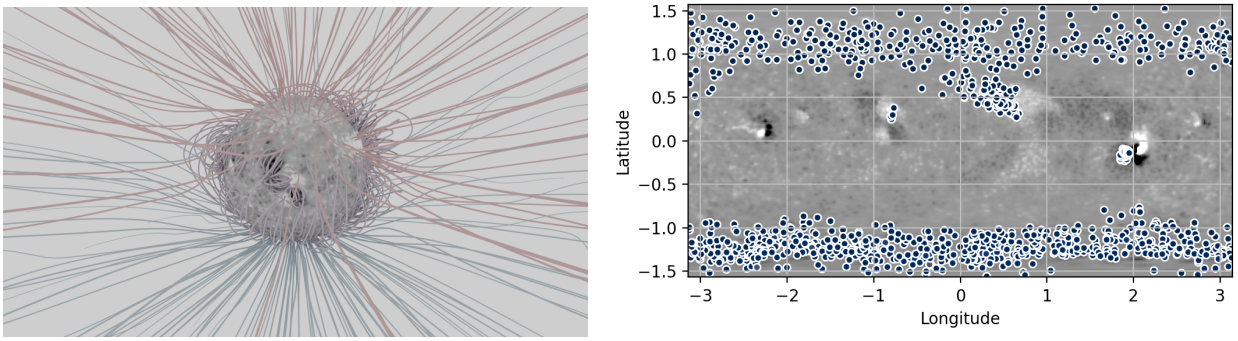

Figure 6: *morphology of a data-driven fluxon model of the Sun during Carrington Rotation 2193 shows high fluxon density (left) and appropriate open-field-line locations (right) after overcoming some difficulties with numerical scaling in Y6. The entire map is covered with fluxons at equal or higher density; only open fluxons are shown, to avoid completely obscuring the magnetogram.*

In the final months of the project, after the Y6 annual report was submitted, we identified and resolved an algorithmic issue that perturbed magnetic results. Because fluxon models in general (and FLUX in particular) treat the magnetic field as a collection of discrete field lines, local discrete geometry of the neighborhood of each fluxon is important. This importance is irreducible: adding more fluxons to a particular simulation refines the grid but retains the low-order polyhedral nature of the neighborhood around each fluxon. We found that the analytic field results could, under certain circumstances, change by a factor of up to 30% between hexagonal-neighborhood fluxons and pentagonal-neighborhood fluxons in force equilibrium in the same domain. The issue turned out to be in the treatment of gradients: while the magnetic field calculation was and remains sound, the treatment of spatial gradients implicitly assumed the same number of sides to each neighboring polygonal domain between fluxon. The issue appears resolved in current versions of the code.

The final result of the development effort is that FLUX is now ready to be used for MHD simulations of CMEs in a background solar wind, and has achieved meaningful data-driven, low-beta 3D MHD simulations of the entire corona with resolution sufficient to capture CME

source region. These simulations can be run in a single workstation rather than a supercomputing cluster, and take hours rather than weeks to complete.

Although we were unable to complete the planned simulations of particular CMEs, we have indeed moved toward inserting magnetic ejecta into a space weather model. We will continue to advance FLUX development and deployment under separate funding.

The FLUX model is available from github: http://github.com/clowder.

References

DeForest, C.E., de Koning, C.A., and Elliott, H.A. 2017: "3D Polarized Imaging of Coronal Mass Ejections: Chirality of a CME", Astrophys. J. 850, 130.

de Koning, C.A. and DeForest, C.E. 2018: "Using Polarized White Light Triplets Measured by STEREO to Isolate Internal Structure", Proc. SHINE-2018.

Howard, T.A. and Pizzo, V.J. 2016: "Challenging Some Contemporary Views of Coronal Mass Ejections. I. The Case for Blast Waves", Astrophys. J. 824, 92.

Howard, T.A., DeForest, C.E., Schneck, U.G., and Alden, C.R. 2017: "Challenging Some Contemporary Views of Coronal Mass Ejections. II. The Case for Absent Filaments", Astrophys. J. 834, 86.